FABAD J. Pharm. Sci., 48, 3, 359-372, 2023
Doi: 10.55262/fabadeczacilik.1187620
RESEARCH ARTICLE

Design and Assessment of a Microemulsion-Based Transdermal Drug Delivery System for Meloxicam; Examination of Formulation Ingredients

Anayatollah SALIMI[*], Ramin NOORAFROOZ[**], Maryam FOULADI[***], Saeed Mohammad SOLEYMANI[****°]

Design and Assessment of a Microemulsion-Based Transdermal Drug Delivery System for Meloxicam; Examination of Formulation Ingredients

SUMMARY

The goal of creating meloxicam-loaded microemulsion formulations was to increase meloxicam permeability through the skin. Using pseudo-ternary phase diagram construction and full factorial design, eight formulations with three independent variables (water percent, oil percent, and surfactant/co-surfactant percent) were selected to be prepared. This research evaluated the formulation's characteristics, including droplet size, viscosity, and release profile. FT-IR and DSC techniques were also utilized to investigate the effect of microemulsion components on rat abdomen skin, and the permeability of meloxicam-loaded microemulsions via rat abdomen skin was also evaluated by calculating permeability parameters such as J_{ss}, D_{app}, T_{lag}, ER_{flux}, ERD, and ERP. When compared to a saturated aqueous solution of meloxicam as a reference, the findings showed that all microemulsion (ME) formulations considerably increased meloxicam permeability through rat skin. Water percent had a direct and significant relationship with J_{ss}, and oil percent had a direct and significant relationship with D_{app}, according to analysis regression. ME components also caused alterations in the skin's lipoprotein bilayers, which might enhance formulation permeability through the skin.

Key Words: *Meloxicam, Microemulsion, Formulation, NSAID, Permeability*

Meloksikam için Mikroemülsiyon Tabanlı Transdermal İlaç Taşıyıcı Sistemin Tasarımı ve Değerlendirilmesi; Formülasyon Bileşenlerinin İncelenmesi

ÖZ

Meloksikam yüklü formülasyonların geliştirilmesindeki amaç meloksikamın deri permeabilitesinin artırılmasıdır. Hazırlamak üzere üçgen faz diyagramı yorumlaması ve tam faktöriyel tasarım kullanılarak üç bağımsız değişken (su yüzdesi, yağ yüzdesi ve sürfaktan/ko-sürfaktan yüzdesi) içeren sekiz formülasyon seçilmiştir. Bu araştırma, damla boyutu, viskozite ve salım profili de dahil olmak üzere formülasyonun karakteristiklerini değerlendirmiştir. Mikroemülsiyon bileşenlerinin sıçan abdomen derisi üzerine etkisini incelemek için FT-IR ve DSC teknikleri de uygulanmış ve meloksikam yüklü mikroemülsiyonların sıçan abdomen derisinden permeabilitesi Jss, Dapp, T1ag, ERakı, ERD ve ERp permeabilite parametreleri hesaplanarak değerlendirilmiştir. Referans olarak meloksikamın doygun sulu çözeltisi ile karşılaştırıldığında sonuçlar tüm mikroemülsiyon (ME) formülasyonlarının meloksikamın sıçan derisinden permeabilitesini büyük ölçüde artırdığını göstermiştir. Analiz regresyonuna göre su yüzdesinin Jss ile ve yağ yüzdesinin Dapp ile direkt belirgin bir ilişkisi vardır. ME bileşenleri ayrıca derinin lipoprotein çift tabakasında değişikliklere neden olarak formülasyonun deriden permeasyonunu artırabilir.

Anahtar Kelimeler: *Meloksikam, Mikroemülsiyon, Formulasyon, NSAİİ, Permeabilite*

Received: 11.10.2022
Revised: 1.03.2023
Accepted: 2.03.2023

[*] ORCID: 0000-0003-1505-7969, Department of Pharmaceutics, Faculty of Pharmacy, Ahvaz Jundishapur University of Medical Sciences, Ahvaz, Iran., Nanotechnology Research Center, Ahvaz Jundishapur University of Medical Sciences, Ahvaz,
[**] ORCID: 0000-0000-0000-0000, Department of Pharmaceutics, Faculty of Pharmacy, Ahvaz Jundishapur University of Medical Sciences, Ahvaz, Iran
[***] ORCID: 0000-0000-0000-0000, Department of Pharmaceutics, Faculty of Pharmacy, Ahvaz Jundishapur University of Medical Sciences, Ahvaz, Iran.
[****] ORCID: 0000-0003-1462-3930, Department of Clinical Pharmacy, School of Pharmacy, Shahid Beheshti University of Medical Sciences, Tehran, Iran.

[°] Corresponding Author; Saeed Mohammad SOLEYMANI
Telephone number: +98-21-66355959,Email Address: mamsoloni@gmail.com

INTRODUCTION

Transdermal medication delivery is a painless, self-administered mode of administration that improves patient compliance. This method of administration allows for long-term release and is often low-cost to prepare (Prausnitz, & Langer, 2008).

Meloxicam is a zwitterion nonsteroidal anti-inflammatory drug (NSAID) made from enolic acid, which at physiological pH is nearly insoluble in water. Meloxicam is classified as a Class II molecule by the Biopharmaceutics Classification System, with a logp = 3.43 and poor solubility and high permeability (Mason, Moore, Edwards, Derry, & McQuay, 2004). NSAIDs are among the most frequently prescribed medications in the world, and they are responsible for around one-fourth of all side effect reports (McNeill, Potts, & Francoeur, 1992). Giving the medication through the skin is one strategy to reduce systemic toxicity, prevent gastrointestinal distress, and have a more effective therapeutic outcome (McNeill, Potts, & Francoeur, 1992; Mason, Moore, Edwards, Derry, & McQuay, 2004). Some of the transdermal formulations of meloxicam that have been developed include liposomes, transferosomes, proniosomes, and gels (Kogan, & Garti, 2006; Lawrence, & Rees, 2012; Čižinauskas, Elie, Brunelle, & Briedis, 2017; Soleymani, & Salimi, 2019). Each of these formulations has its own set of benefits and drawbacks; for example, liposomes and transferosomes are both chemically unstable and costly (Lapina, Vorobey, Pavich, & Opitz, 2013; Solanki, Kushwah, Motiwale, & Chouhan, 2016).

Microemulsions are translucent, thermodynamically stable liquids made up of water, oil, and surfactants (Salimi, Moghimipour, & Tavakolbekhoda, 2013). Depending on the components of the microemulsion, these formulations may improve the transdermal distribution of both hydrophilic and lipophilic drugs (Moghimipour, Salimi, & Zadeh, 2013). These formulations have several benefits, including ease of production, minimal preparation costs, high drug capacity, and thermodynamic stability (Kogan, & Garti, 2006).

In this investigation, we prepared and characterized eight meloxicam-loaded microemulsions with three independent variables including water percent (5% and 10%), oil percent (5% and 50%), and surfactant/co-surfactant ratio (1:1 and 3:1) and evaluated dependent variables such as droplet size, viscosity, release percent, and permeability parameters. A DSC and an FT-IR method can also be used to look at how the microemulsion components affect the meloxicam permeability and the structure of the skin of rats.

MATERIALS AND METHODS

Materials

Meloxicam was purchased from Iran Hormone pharmaceutical company (Tehran, Iran). We received gift samples of diethylene glycol monoethyl ether (Transcutol P) from the Gattefosse company (France). Purchases from the Merck Company included tween80, span20, propylene glycol, oleic acid, potassium phosphate monobasic, and dibasic (Germany).

Methods

Solubility test in components of the formulation

Meloxicam's solubility in two oils (Transcutol P, oleic acid), surfactants (Tween-80 and span 20), and cosurfactants were determined (propylene glycol). A surplus of meloxicam was added to 5 ml of each chosen solvent, which was then agitated at 20 °C for 48 hours before being centrifuged for 5 minutes at 8000 rpm. For removing the undissolved drug, centrifugation was performed at 8000 rpm for 30 minutes, the supernatant was filtered through a membrane filter (0.22mm), extracted with methanol solvent, and the amount of meloxicam in the methanol was evaluated

by UV spectroscopic analysis (Moghimipour, Salimi, & Zadeh, 2013).

Animals

In the *in vitro* permeation study, eight male Wistar rats weighing 200-250 g were utilized. The abdomen skin hair was meticulously cut with an electric clipper and razor following the animal's slaughter under anesthesia with 50/10 mg/kg ketamine/xylazine. When the skin was dissected, any additional subcutaneous fat from the dermal surface was eliminated. Until they were required for the permeability experiments, the skin samples were stored at -20° C in a freezer. All of the skin samples had a thickness of roughly 0.8mm. This work received ethical approval from the Jundishapur University of Medical Sciences ethics committee (IR.AJUMS.ABHC.REC.1398.053) (Golden, Guzek, Harris, McKie, & Potts, 1986).

Construction of pseudo-ternary phase diagrams

By titrating a series of three-component surfactant-cosurfactant-oils in an aqueous solution at room temperature, the pseudo-ternary phase diagrams were created. Two-phase diagrams were created using the mass ratios of (Tween80-Span 20/PG) of 1:1 and 3:1, respectively. The oil phase (Oleic acid-Transcutol-P) (10:1) and the surfactant mixture were then combined in each phase diagram at the following mass ratios: 1:9, 2:8, 3:7, 4:6, 5:5, 6:4, 7:3, and 9:1. At 25±1oCand with moderate agitation, these combinations were diluted dropwise with double distilled water. Each ternary system's component % composition was calculated, and the observed results were plotted on triangular coordinates to create the phase diagrams. Table 1 lists the components used in the formulation of microemulsions.

Table 1: Composition of prepared microemulsions of meloxicam

Formulation	Factorial	S/C	% S + C	% Oil	%W
ME1	+ + +	3:1	40	50	10
ME2	- + +	3:1	45	50	5
ME3	+ - +	3:1	85	5	10
ME4	- - +	3:1	90	5	5
ME5	+ - -	1:1	85	5	10
ME6	- - -	1:1	90	5	5
ME7	- + -	1:1	45	50	5
ME8	+ + -	1:1	40	50	10

Meloxicam MEs preparation

After the ME boundary in the phase, diagrams were defined, and eight ME formulations were created using the full factorial design with the three variables at two levels. The surfactant/co-surfactant ratio (S/Co), the percentage of oil (percent Oil), and the percentage of water are the key factors considered in calculating the quantities of ME components (percent W). To create MEs, eight ME samples with varying amounts of oil (5% and 50%), water (5% and 10%), and the S/Co ratio (1:1 and 3:1) were selected. The pseudo-ternary phase diagram was used to create several MEs using 1:1 and 3:1 mass ratios of Tween 80: Span 20/propylene glycol. Drop by drop, meloxicam (0.3%) was incorporated into the oily phase with the required amount of double distilled water, and S/Co was blended by rapidly stirring the mixtures at room temperature until a clear liquid was created.

Measurement of droplet size

The droplet size of each microemulsion formulation was determined by a nanodroplet size analyzer at 25°C.

Viscosity measurements

The viscosity of samples was measured at 25 °C with a Brookfield viscometer (DV-II+Pro Brookfield, USA) using spindle no. 34 at a rotational speed of 50 and 100 rpm. Each measurement was performed in triplicate.

Release study

The release rate of meloxicam from several microemulsion formulations was measured using Franz diffusion cells with a cellulose membrane (12 kD, an area of 3.4618 cm^2). At 25 degrees Celsius, the cellulose membrane was immersed overnight in distilled water. The donor and receptor compartments of the cells were then separated by a membrane that was clamped between them. 25 mL of phosphate buffer (pH = 7.4) was added to each Diffusion cell. Throughout the experiment, the receptor fluid was churned at 200 rpm by externally powered magnetic bars. Meloxicam microemulsion (5g) was weighed precisely and deposited in the donor compartment. The fresh receptor medium was replaced immediately with an equivalent amount of sample after 0.5, 1, 2, 3, 4, 5, 6, 7, 8, and 24 hours after application. A UV-visible spectrophotometer at 362nm was used to evaluate the samples. The data was shown as a proportion of total released drugs over time (Soleymani, & Salimi, 2019).

Skin permeation study

The Franz diffusion cell with a diffusion area of 3.4618 cm2 and a receptor volume of 25 ml was utilized to conduct permeation tests on the rat skins. The pH 7.4 phosphate buffer was poured into the receptor compartment. The diffusion cells were placed on a heater stirrer (37 ± 0.5 °C) and the receptor phase was stirred continuously at 200 rpm using small magnetic bars. After that, a meloxicam-loaded microemulsion (5g) was applied to the skin's epidermal surface. At 0.5, 1, 2, 3, 4, 5, 6, 7, 8, 12, and 24 hours following the administration, 2 mL of the receptor compartment was sampled. After each sample, an equivalent amount of new phosphate buffer was immediately supplied until sink conditions were achieved. UV spectroscopy at 362 nm was used to determine the concentrations of the samples. Each formulation was put through three rounds of testing (Soleymani, & Salimi, 2019).

Statistics and data analysis

The total amount of meloxicam that penetrated the receptor via each unit area of the diffusion surface was determined and displayed as a function of time. The linear portion of the permeation curve's slope was used to compute steady-state flux (mg/cm^2.h). The permeability coefficient (K_p, cm/h) of meloxicam through the skin was determined using Equation 1**:**

$$K_p = \frac{J_{ss}}{C_v} \qquad \text{(Equation 1)}$$

Where Jss and Cv are steady-state flux and initial concentration of caffeine in the receptor compartment, respectively**.**

Enhancement ratios (ER) were calculated from equation 2**:**

$$ER = \frac{permeability\ parameter\ after\ treatment}{permeability\ parameter\ before\ treatment} \qquad \text{(Equation 2)}$$

One-way ANOVA was used for the statistical comparison, and $p<0.05$ was taken into account as statistically significant.

Effect of ME components on skin permeability

For the pretreatment of skin samples, fully hydrated samples were pretreated by putting 2 ml of microemulsion components on the surface of the skin in the donor phase. The donor and receptor compartments were then washed with water and filled with an aqueous solution of meloxicam and phosphate buffer (pH 7), respectively. The effect of ME compo-

nents (Transcutol p, oleic acid, PG, span 20, tween 80) was evaluated for meloxicam permeation through whole skin samples. At 0.5, 1, 2, 3, 4, 5, 6, 7, 8, 12, and 24 hours following the administration, 2ml of the receptor compartment was sampled. After each sample, an equivalent amount of new phosphate buffer was immediately supplied until sink conditions were achieved. UV spectroscopy at 362 nm was used to determine the concentrations of the samples (Soleymani, & Salimi, 2019).

FT-IR experiments

The excised abdominal rat skin samples were treated for 24 hours with oleic acid, transcutol p, Tween 80, span 20, and propylene glycol, then vacuum-dried (650 mm Hg, 25±1°C) for 1 hour and kept in desiccators to evaporate component traces. An FT-IR was used to scan the skin samples measuring between 4,000 and 500 cm^{-1} (Soleymani, & Salimi, 2019).

Differential scanning calorimeter (DSC)

A DSC (DSC system, Mettler Toledo) was used to investigate changes in the structure of whole skin-induced ME components. The completely hydrated skin samples were first soaked in ME components for 24 hours and then blotted dry before being hermetically sealed to prevent water evaporation. Pretreated skin samples weighing 6–10 mg were placed within aluminum pans that were hermetically sealed. An empty pan that had been hermetically sealed was also used as a comparison. Temperatures of 20 to 200 °C were applied to skin samples (scan rate: 50 C/min). Every experiment was performed at least three times (Soleymani, & Salimi, 2019).

RESULTS

Construction of pseudo-ternary phase diagrams

Figure 1 shows the Pseudo ternary phase diagrams of oleic acid: Transcutol P/Tween 80: Span 20/Propylene glycol/Water.

The obtained three-phase diagrams with a surfactant to the co-surfactant ratio of 3:1 and 1:1 are shown in Fig. 2 and Fig. 3 respectively.

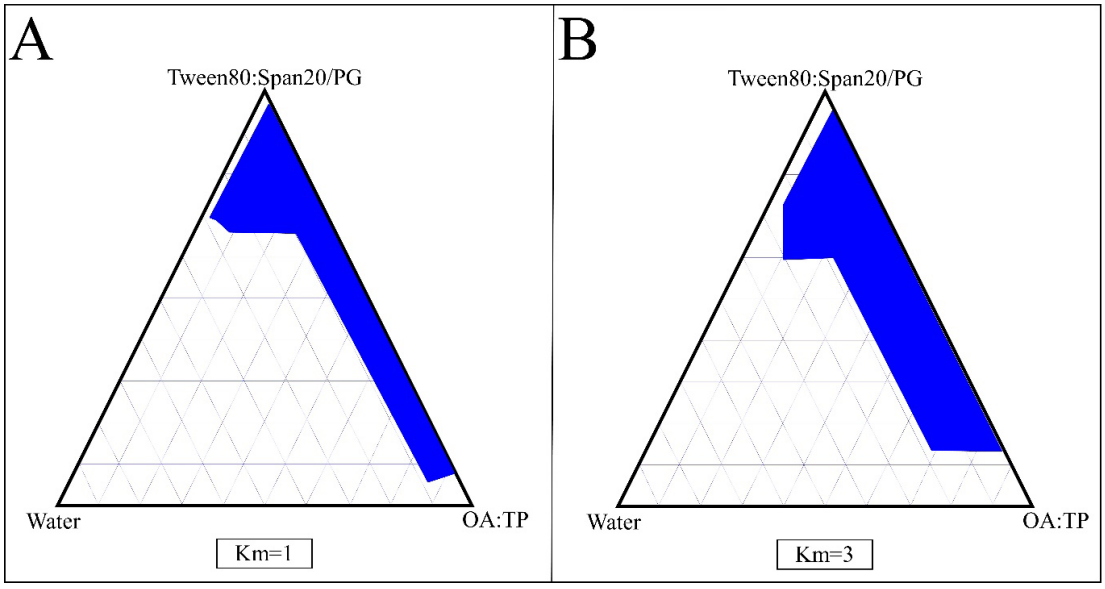

Figure 1. The Pseudo Ternary Phase Diagrams of the Oil-surfactant/Cosurfactant Mixture-water System at the 1:1 and 3:1 Weight Ratio of Tween 80/Span 20/PG at Ambient Temperature, Dark Area Show MEs boundary

Microemulsion droplets droplet size

Prepared microemulsion formulations were characterized and their characteristics including droplet size, viscosity, and drug release were evaluated. The measured droplet size of each formulation is shown in Table 2. The droplet size of the microemulsion formulations was in the range of 5.24 to 16.75 nm and there was not any relationship between independent variables and the droplet size.

Table 2: Droplet size of the prepared formulations (Mean±SD, n=3).

Formulation	Droplet size (nm)
ME1	7.30±0.03
ME2	9.74±0.58
ME3	12.3±0.42
ME4	16.75±0.15
ME5	5.24±0.31
ME6	7.55±0.41
ME7	8.16±0.12
ME8	12.7±0.3

Viscosity of MEs

The measured viscosities of prepared formulations are shown in Table 3. The microemulsion formulation's viscosity was in the range of 132 to 418 cps.

Table 3: Viscosity of meloxicam ME formulations at 50 and 100 rpm rate (Mean±SD, N=3)

Formulation	Viscosity with a 50rpm rate (cps)	Viscosity with a 100rpm rate (cps)
ME1	156.5±1.4	132±1.6
ME2	169.5±0.87	145±1.4
ME3	392±1.2	400±1.45
ME4	411.5±1.97	418±1.7
ME5	249±1.37	252±1.84
ME6	248±0.61	249±0.9
ME7	219±1.6	175±1.75
ME8	163.5±1.83	112.5±1.11

Released drug from ME formulations

The evaluation of released medications from microemulsion formulations is provided in Table 4 and Figure 2.

Table 4: The kinetics of release and meloxicam release percent of the prepared MEs (Mean±SD, n=3).

Formulation	%Release(24h)	Kinetic of Release	r^2
ME1	82.68	Zero	0.997
ME2	56.46	First	0.999
ME3	27.68	First	0.992
ME4	34.37	Higuchi	0.997
ME5	71.20	Zero	0.999
ME6	58.11	First	0.999
ME7	94.29	Higuchi	0.990
ME8	92.48	3/2 root of mass	0.997

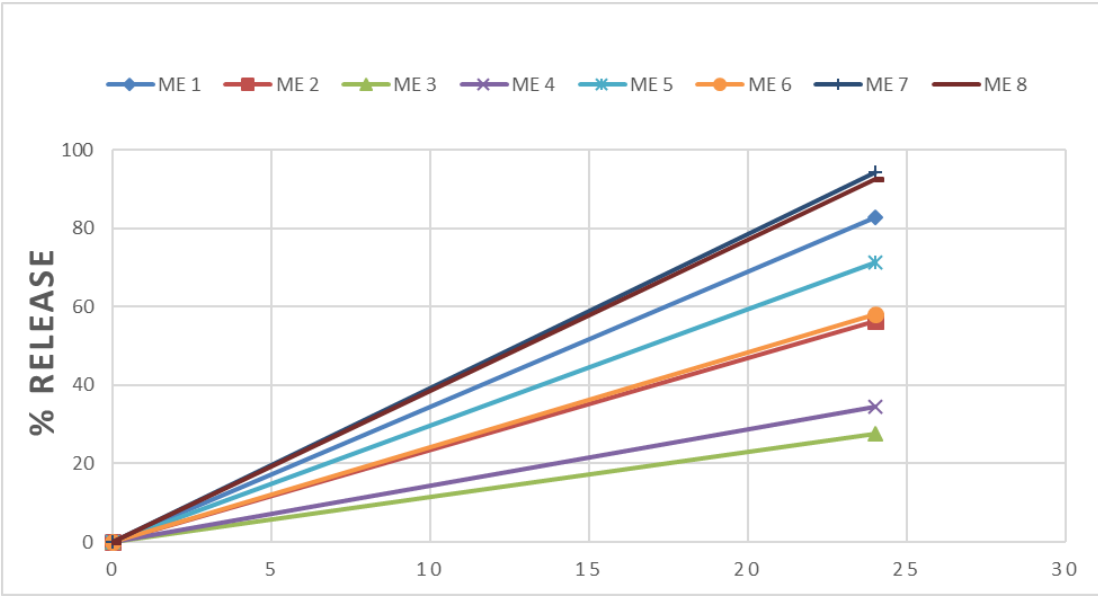

Figure 2. Release percentage of meloxicam from microemulsions after 24 hours.

Meloxicam skin permeability

In addition to the physicochemical properties of microemulsion formulations, their permeability through rat skin was also evaluated. Table 5 shows the permeability characteristics of several meloxicam microemulsions. Meloxicam permeation patterns through removed rat skins from MEs are shown in Figure 2. The permeability of meloxicam-loaded ME formulations through the skin of rats was assessed, and permeability metrics such as the permeation rate in steady state (Jss), permeability coefficient (P), lag time (T_{lag}), and apparent diffusion coefficient (Dapp) were computed. Table 5 shows that ME2 and ME6 had the highest and lowest ERP and ERflux, respectively.

Table 5. The Permeability Parameters of Different ME Formulations of Meloxicam through the Rat Skin (Mean±SD, n=3).

Formulation	J_{ss}(mg/cm².h)	D_{app}(cm²/h)	P(cm/h)	T_{lag}(h)	**ER_{flux}**	**ER_D**	**ER_p**
Control	0.0036±0.0003	0.0021±0.0001	0.0012±0.0002	35.612±21.538	-	-	-
ME1	0.0517±0.0001	0.0248±0.004	0.0172±0.0	2.05±0.230	14.361±2.6	11.809±1.2	14.333±1.4
ME2	0.0744±0.001	0.0075±0.001	0.0248±0.002	6.565±0.202	20.649±3.6	3.571±0.353	20.650±3.2
ME3	0.0618±0.002	0.0244±0.002	0.0206±0.002	2.664±0.096	17.166±1.1	11.619±0.9	17.145±1.1
ME4	0.0501±0.002	0.0453±0.008	0.0167±0.001	1.239±0.115	13.897±2.3	21.567±1.1	13.916±2.3
ME5	0.0528±0.002	0.006±0.0001	0.0176±0.003	8.957±0.541	14.641±0.6	2.851±0.1	14.612±0.6
ME6	0.023±0.002	0.01±0.0005	0.007±0.0001	4.856±0.116	6.388±0.5	4.761±0.4	5.831±0.7
ME7	0.0727±0.003	0.0273±0.001	0.0242±0.001	2.527±0.231	19.916±2.6	11.285±1.7	20.147±1.2
ME8	0.0661±0.001	0.007±0.0	0.022±0.001	7.986±0.002	18.341±1.3	3.315±1.9	18.290±1.4

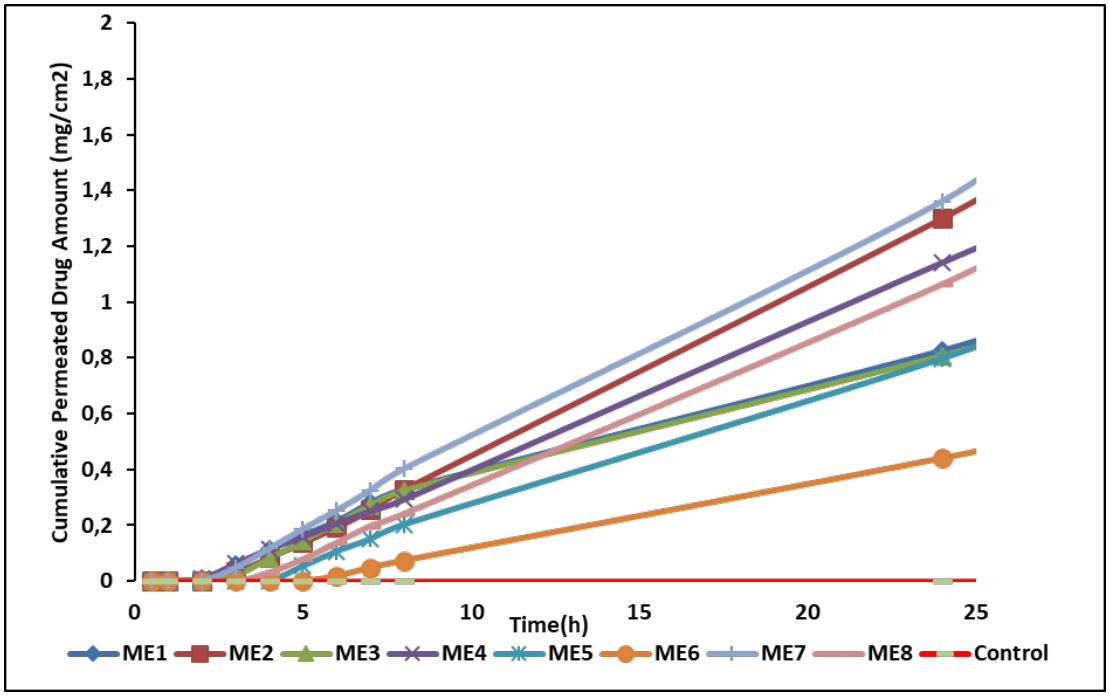

Figure 3. Permeation Profiles of Meloxicam from Various microemulsion Formulations Through Excised Rat Skin

Effect of microemulsion components on skin permeability and rat skin structure

Permeability parameters of meloxicam after pretreatment with components were shown in tables 6 and 7.

Table 6. Permeability parameters of meloxicam after pretreatment with components compared to control (Mean ± SD, n = 3)

Component	J_{ss}(mg/cm².h)	D_{app}(cm²/h)	P(cm/h)	T_{lag}(h)
Control	0.00002±0.0036	0.0001±0.0021	0.0002±0.0012	2.5±35.6
Oleic Acid	0.0007± 0256.0	0.0004± 0073.0	0.0002± 0.0085	0.75 ± 10.87
Transcutol-p	0.0002± 0.0416	0.0008± 0.0176	0.0003± 0.0138	0.9 ± 3.45
PG	0.0002± 0.0447	0.0002± 0.0062	0.0001± 0.0149	0.1± 9.7
Span 20	0.0001± 0.0691	0.0004± 0.01	0.0002± 0.023	0.9± 5.93
Tween 80	0.0003± 0.086	0.0006± 0.0058	0.003 ± 0.028	0.04 ± 5.67

Table 7. Effect of components on derived permeation parameters for meloxicam (mean ± SD, n = 3)

Component	ER_{flux}	$_{E}RD$	ER_{p}
Oleic Acid	0.074± 7.068	0.045± 3.416	0.216 ± 7.08
Transcutol	0.087±11.345	0.06± 2.39	0.005 ±11.573
PG	0.168±12.398	0.124± 2.285	0.231±12.361
Span 20	0.147±19.181	0.06± 4.719	0.216±19.156
Tween 80	0.341±23.782	0.147±2.732	0.634±23.124

Evaluation of component's effect on rat skin by FT-IR

Tables 8-10 shows the obtained data from FT-IR spectrums of treated skin with different microemulsion formulation components.

Table 8. FT-IR Peak wave numbers (cm^{-1}) change after treatment with various microemulsion formulation ingredients in comparison to control (untreated skin) and abdominal entire skin rats. (mean ± SD, n = 3)

Components	Asymmetric C-H stretching	Symmetric C-H stretching	C=O stretching of lipid ester	C=O stretching Of keratin (Amide I)	C=O stretching of lipid ester (Amide II)
Control	2948.02±0.115	2821.65±0.42	1723.65±0.55	1652.78±0.35	1572.27±0.12
PG	2910.5±0.012	2848.3±0.11	1794.003±0.14	Deleted	Deleted
Span 20	2938.83±0.11	2830.72±0.06	Deleted	1675.84±0.38	1504.9±0.62
Tween 80	2901.75±1.02	Deleted	1732.18±0.19	1917.7±0.9	Deleted
Oleic acid	Deleted	2858.015±1.2	Deleted	1822.54±0.56	1462.82±0.72
Transcutol- p	3068.98±0.35	2845.73±1.4	Deleted	1694.45±0.8	1433.47±0.63

Table 9. The abdominal entire skin of rats treated with various microemulsion formulation ingredients showed a decrease in the mean peak height of asymmetric (Asy) and symmetric (Sym) C-H stretching and C=O stretching absorbance when compared to the control (untreated skin). (mean±SD, n=3)

components	**Asymmetric C-H stretching**		**Symmetric C-H stretching**		**C=O stretching of lipid ester**	
	Peak height	**%D**	**Peak height**	**%D**	**Peak height**	**%D**
Control	4.877±0.001	-	5.026±0.025	-	4.999±0.006	-
PG	0.172±0.035	96.47	0	100	0.024±0.008	99.51
Span 20	2.66±0.025	45.45	2.425±0.041	51.75	0	100
Tween 80	0.493±0.066	89.89	0	100	0.096±0.025	98.07
Oleic acid	0	100	0.716±0.114	85.17	0	100
Transcutol- p	0.634±0.041	87	0.67±0.017	56.66	0	100

*%Decrease in peak height(%D) =(peak height from hydrated whole skin - peak height from component treated whole skin)/ peak height from hydrated whole skin x 100

Table 10. Decrease in mean peak height compared with control (untreated skin) of C=O stretching (Amide I) and C-N stretching of keratin(Amide II)absorbance of abdominal whole skin rat following treatment with different microemulsion formulation components. (mean ± SD, n = 3)

Components	C=O stretching	Of keratin	C-N stretching	Of keratin
	Peak height	% D	Peak height	% D
Control	4.952±0.021	-	4.84±0.045	-
PG	0.172±0.004	96.52	0	100
Span 20	1..938±0.001	60.86	1.741±0.045	64.02
Tween 80	0.008±0.001	99.83	0	100
Oleic acid	1.087±0.026	78.04	0.954±0.013	80.28
Transcutol- p	1.051±0.024	78.77	1.151±0.018	76.21

Evaluation of component's effect on rat skin by DSC method

Table 11 displays the rat skin's phase transition temperature movement and enthalpy values following treatment with various components.

Table 11: Effect of microemulsion components on the thermal properties of whole abdominal rat skin (mean ± SD, n = 3)

Components	Phase transition temperature		Enthalpy	
	Tm1	$_{T}$m2	ΔH_1	ΔH_2
Water	67.5±2.1	112±6.6	-7.01±0.4	-555.1±19.5
PG	Deleted	89±5.9	Deleted	11.51±2.2
Oleic acid	51±0.63	135±2.6	0.45±0.002	25.47±1.92
Transcutol-p	48±2.12	117±1.2	0.23±0.039	35.61±2.4
Tween 80	Deleted	Deleted	Deleted	Deleted
Span 20	Deleted	97±1	Deleted	3.014±0.012

DISCUSSION

Surfactant and co-surfactant mass ratios are critical characteristics that influence the behavior of phase diagrams in MEs. Previous research has shown that increasing the relative amount of the surfactant component increases the size of the ME region. (Lawrence & Rees, 2000) By increasing the surfactant to co-surfactant mass ratio of 3:1 and 1:1, the ME limits were enlarged.

The obtained droplet sizes demonstrate that the maximum and minimum droplet sizes are related to formulation numbers 4 and 5 respectively.

Regression analysis indicates that there is a significant and inverse relation between viscosity and water percent (P = 0.001). It means that an increase in water percent decreases the viscosity of microemulsion. Also, a significant and direct relationship between the oil percent and viscosity of the formulations (P = 0.038). In other words, an increase in oil percent increases the viscosity of formulations. Results from Table 3 demonstrate that in low levels of oil, an increase in water percent from 5 to 10 caused a decrease in the viscosity of microemulsion formulations, and in high levels of oil, an increase in

water caused a more significant decrease in viscosity. The formulations with the highest and lowest viscosity are ME 4 and ME1, respectively.

Maximum and minimum released drug percent is related to formulation ME7 and ME3 with percent of 94.29 and 27.68 % respectively. The S/C ratio has no relationship with drug release percent (P = 0.723), but the percentage of medication release and the percentage of oil has a clear and significant relationship. (P = 0.001), as well as a direct and significant relationship between drug release percent and oil percent (P = 0.001). This suggests that increasing the percentage of oil in a microemulsion formulation improves medication release.

There is a clear difference in the flux of meloxicam ME formulations and meloxicam saturated solution as control into rat skin. Maximum flux was observed by ME2 with 0.3% drug, 50% oil phase, 5% aqueous phase, and 45% surfactant and co-surfactant mixture. there is a direct and significant relationship between flux and water percent as well as an increase in water percent increased flux. Based on the permeability results, the maximum permeability coefficient (P) and maximum Tlag are related to ME2 and ME5 respectively. In addition, ME4 showed a diffusion coefficient (Dapp) with a value of 21.567 times higher than the drug-saturated aqueous solution. Regression analysis demonstrates significant relation between the Jss, P, and Dapp and independent variables. It showed that there is a significant and direct relation between the water percent and Jss and P and also a significant and direct relation between the oil percent and Dapp. It seems that a reduction in ME viscosity by the increase in water percent, enhanced the drug release rate from MEs and this resulted in the enhancement of drug permeation rate (JSS). On the other hand, regression analysis showed that oleic acid as an oil phase is in inverse relation with Tlag. It seems that oleic acid, as the oil phase disordered the lipoprotein bilayers in SC which cause the weakness of the lipoprotein structure. The penetration enhancers increase drug permeability by enhancement in diffusion and distribution coefficient (Čižinauskas, Elie, Brunelle, & Briedis, 2017). Generally, permeation studies demonstrate that all ME formulations could increase meloxicam permeability through rat skin significantly comparing the saturated aqueous solution of meloxicam. This result was also obtained by several other conducted studies to enhance the transdermal permeation of different pharmacological compounds including Thai mango seed kernel extract, *Houttuynia cordata*, and celecoxib (Salimi, Moghimipour, & Tavakolbekhoda, 2013; Leanpolchareanchai, Padois, Falson, Bavovada, & Pithayanukul, 2014; Pang, Dong, Li, Xia, Liu, Hao, & et al. 2017).

FTIR was used to conduct a molecular analysis of the entire rat skin to better understand the mechanism by which the characteristics of components and retardants change in a specific media (Soleymani, & Salimi, 2019). The movement of protein and lipid molecules in the SC causes many of the infrared spectral bands to appear on the skin. A good indicator of the lipid architecture of lamellae is lipid vibration in the intercellular region of the SC layer. SC stretching vibrations of CH_2 symmetric (about 2850 cm^{-1}) and CH_2 asymmetric (approximately 2920 cm^{-1}) vibrations were found. The quantity and width of CH_2 stretching rise increase when the lipids in the stratum corneum fluidize. If the shift is blue, it means the SC membrane (lipid bilayer) is fluidizing, causing the barrier properties to break down, allowing more material to pass through the SC. In contrast, lipid groups reorient, resulting in a change in wavenumber (e.g., a redshift) and strengthening of subcutaneous barrier characteristics, reducing permeant transit through the skin. The band location (wavenumber) of the signals at 2920, 2850, and about 1738 cm^{-1} rises or decreases as the ME component acts on the lipid pathway, showing

a phase shift of the lipids. In the spectrum analysis, peak wavenumber positions and intensities between 4000 cm-1 and 500 cm-1 were examined (Table 9-11).

According to the findings, hydrated rats' skin(-control) displayed peak locations. at 3105.44 cm^{-1}, 3200.08 cm^{-1}, 3255.3 cm^{-1}, 3310.2 cm^{-1}, 3417.59 cm^{-1}, 3610.46 cm^{-1}, 2947.8 cm^{-1}, 2821.6 cm^{-1}, 1723.66 cm^{-1}, 1652.78 cm^{-1} and 1572.27 cm^{-1} area.

Peak positions near 2947.8 cm-1(CH2 symmetric) and 2821.6 cm^{-1} (CH2 asymmetric) areas indicate bands related to terminal methyl groups of the lipids in the skin. In addition, Peak positions in 1652.78 cm^{-1} and 1572.27 cm^{-1} indicate type 1 amide (C=O group) and type 2 amide (C-N group) in keratin helix secondary structure respectively (Obata, Utsumi, Watanabe, Suda, Tokudome, Otsuka, & Takayama, 2010; Moghimipour, Salimi, & Zadeh, 2013).

The C=O stretching of the lipid ester band area and the asymmetric C-H stretching band region are missing in the FT-IR spectra of oleic acid-treated skin. In addition, in both the symmetric C-H stretching and the amide I regions, peak locations demonstrate a rise in absorption wavelength. This implies a blue shift in liquefaction in the stratum corneum's bilayers.

The Tween 80-treated entire skin rat's IR spectra showed substantial reductions in peak height at all wave numbers. In SC, an increase in permeability parameter was seen following skin pretreatment with tween 80, with effects on the lipid bilayer and protein pathway.

In the FT-IR spectra of transcutol-p treated skin, the C=O stretching of the lipid ester band region is lacking. Peak positions show an increase in absorption wavelength in both the asymmetric C-H stretching and symmetric C-H stretching areas, as well as the amide I region. The IR spectra of the transcutol-p-treated whole skin rat exhibited significant decreases in peak height at all wave numbers. This indicates a blue shift in liquefaction in the bilayers of the stratum corneum. Following skin pretreatment with transcutol-p, an increase in permeability parameter was seen in SC, with effects on the lipid bilayer and protein pathway.

The C=O stretching of the lipid ester band area is absent from the FT-IR spectra of span-20-treated skin. In both the symmetric C-H stretching sections as well as the amide I region, peak locations demonstrate an increase in absorption wavelength. The stratum corneum bilayers have a blue shift in liquefaction. At all wave numbers, the peak height of the IR spectra of the span20-treated entire skin rat was significantly reduced. After span 20 was put on the skin, the SC permeability parameter went up. This could affect the lipid bilayer and the way proteins move through it.

In the FT-IR spectra of propylene glycol-treated skin, the amide I band area and the amide II band region is lacking. Peak sites show an increase in absorption wavelength in both the symmetric C-H stretching and the C=O stretching of lipid ester regions. This shows a blue change in liquefaction in the bilayers of the stratum corneum. Propylene glycol made the skin on the SC more permeable. This mostly affected the protein route, but it also made the skin more permeable.

The DSC method is useful for figuring out lipid melting temperatures, lipid bilayer phase transitions, and protein denaturation in horny layers. This technique uses the phase transition average temperature (Tm) and enthalpy value to assess the Thermotropic behavior of skin treated with various components. A decrease in enthalpy value indicates lipid melting of lipid bilayers in the horny layer (Amin, Kohli, Khar, Mir, & Pillai, 2008). Additionally, the lipid layer's irreversible disorder and the horny layer's protein denaturation are both shown by the phase transition temperature moving to a lower temperature.

Based on research findings conducted by Kaushik et al. on the skin horny layer, three endothermic peaks were reported in temperature ranges of 59-63C° (Tm1), 75–82°C (Tm_2), and 99.5–120°C (Tm_3), but an endothermic peak of 35–40 °C was omitted since the skin samples were dried before the DSC test. Observing this peak needs at least 15% moisture in the skin. (16) Tm_1, Tm_2, and Tm_3 are related to the lipid transition temperature from lamellar to disordered structure, the keratin-lipid complex melting point or disorder in the lipid polar head, and proteins' irreversible denaturation in the horny layer, respectively (Golden, Guzek, Harris, McKie, & Potts, 1986; Obata, Utsumi, Watanabe, Suda, Tokudome, Otsuka, & Takayama, 2010).

Based on the obtained data from DSC thermograms, two-phase transitions were observed in the DSC of treated skin with water. The first one was observed at 67.5 C° (Tm_1) and is related to a lipid phase transition, and the second one at 112 C° (Tm_2) is related to irreversible protein denaturation.

Obtained data from DSC thermograms of treated skin with PG demonstrate the elimination of Tm_1, ΔH_1 and also a decrease in Tm_2 and ΔH_2 in comparison with control, which is caused by lipid melting and disordering the protein structure of the bilayer and, consequently, weakness of the lipid structure in lipid bilayers. This mechanism might be quite significant in the increase of meloxicam permeated through rat skin.

DSC thermograms of treated skin with oleic acid and transcutol-p indicate a decrease in Tm_1, ΔH_1, and ΔH_2 which means that these two components cause disordering in lipoprotein bilayers in the skin.

In addition, DSC thermograms of treated skin with tween 80 and span 20 demonstrate the elimination of Tm1 and ΔH_1 and also a decrease in Tm_2 and ΔH_2 (which is more significant in the span 20 thermograms). These changes are caused by lipid melting and disordering of protein structures in the bilayer and, therefore, the weakness of lipid structures in the bilayer.

CONCLUSION

In this study, a meloxicam-loaded microemulsion formulation was created by use of water, oleic acid, tween 80, span 20. Prepared formulations showed significant enhancement in meloxicam permeability in comparison to a saturated aqueous solution of meloxicam. Therefore, this formulation may be a promising carrier for the enhancement of transdermal drug delivery.

ACKNOWLEDGMENT

This article is extracted from PharmD thesis (Fouladi M) and supported by Ahvaz University of Medical Sciences, Jundishapur, Ahvaz.

AUTHOR CONTRIBUTION STATEMENT

A. S. conceived and designed the evaluation and drafted the manuscript. S. M. S. participated in designing the evaluation, performed parts of the statistical analysis, and helped to draft the manuscript. R.N. re-evaluated the clinical data, revised the manuscript and performed the statistical analysis, and revised the manuscript. M.F. collected the clinical data, interpreted them, and revised the manuscript. A.S. re-analyzed the clinical and statistical data and revised the manuscript. Final approval of the version to be published: A. S., R.N., S. M. S., M. F.

CONFLICT OF INTEREST

The authors declare that there is no conflict of interest.

REFERENCES

Amin, S., Kohli, K., Khar, R. K., Mir, S. R., & Pillai, K. K. (2008). Mechanism of in vitro percutaneous absorption enhancement of carvedilol by penetration enhancers. Pharmaceutical development and technology, 13(6), 533-539.

Čižinauskas, V., Elie, N., Brunelle, A., & Briedis, V. (2017). Skin penetration enhancement by natural oils for dihydroquercetin delivery. Molecules, 22(9), 1536.

Golden, G. M., Guzek, D. B., Harris, R. R., McKie, J. E., & Potts, R. O. (1986). Lipid thermotropic transitions in human stratum corneum. Journal of Investigative Dermatology, 86(3), 255-259.

Kogan, A., & Garti, N. (2006). Microemulsions as transdermal drug delivery vehicles. Advances in colloid and interface science, 123, 369-385.

Lapina, V. A., Vorobey, A. V., Pavich, T. A., & Opitz, J. (2013). Targeting diamond nanoparticles into folate-receptor expressing HeLa cells. Journal of Applied Spectroscopy, 80, 414-418.

Lawrence, M. J., & Rees, G. D. (2012). Microemulsion-based media as novel drug delivery systems. Advanced drug delivery reviews, 64, 175-193.

Leanpolchareanchai, J., Padois, K., Falson, F., Bavovada, R., & Pithayanukul, P. (2014). Microemulsion system for topical delivery of thai mango seed kernel extract: development, physicochemical characterisation and ex vivo skin permeation studies. Molecules, 19(11), 17107-17129.

Mason, L., Moore, R. A., Edwards, J. E., Derry, S., & McQuay, H. J. (2004). Topical NSAIDs for chronic musculoskeletal pain: systematic review and meta-analysis. BMC musculoskeletal disorders, 5(1), 1-8.

McNeill, S. C., Potts, R. O., & Francoeur, M. L. (1992). Local enhanced topical delivery (LETD) of drugs: does it truly exist?. Pharmaceutical research, *9*, 1422-1427.

Moghimipour, E., Salimi, A., & Zadeh, B. S. M. (2013). Effect of the various solvents on the in vitro permeability of vitamin B12 through excised rat skin. Tropical Journal of Pharmaceutical Research, 12(5), 671-677.

Obata, Y., Utsumi, S., Watanabe, H., Suda, M., Tokudome, Y., Otsuka, M., & Takayama, K. (2010). Infrared spectroscopic study of lipid interaction in stratum corneum treated with transdermal absorption enhancers. International journal of pharmaceutics, 389(1-2), 18-23.

Pang, J., Dong, W., Li, Y., Xia, X., Liu, Z., Hao, H., ... & Liu, Y. (2017). Purification of Houttuynia cordata Thunb. essential oil using macroporous resin followed by microemulsion encapsulation to improve its safety and antiviral activity. Molecules, 22(2), 293.

Prausnitz, M. R., & Langer, R. (2008). Transdermal drug delivery. Nature biotechnology, 26(11), 1261-1268.

Salimi, A., Moghimipour, E., & Tavakolbekhoda, N. (2013). Transdermal delivery of celecoxib through rat skin from various microemulsions. International research journal of pharmaceutical and applied sciences, 3(4), 173-181.

Salimi, A., Soleymani, H. M., & Soleymani, S. M. (2023). Altered Skin Permeation of Finasteride Using Clove Oil, Urea, and Lyophilized Powder of Grape Seed Extract. Advanced Pharmaceutical Bulletin, 13(1), 96.

Solanki, D., Kushwah, L., Motiwale, M., & Chouhan, V. (2016). Transferosomes-a review. World journal of pharmacy and pharmaceutical sciences, 5(10), 435-449.

Soleymani, S. M., & Salimi, A. (2019). Enhancement of dermal delivery of finasteride using microemulsion systems. Advanced Pharmaceutical Bulletin, 9(4), 584.